 doi:10.20944/preprints202205.0153.v1

Heterogeneities in ventricular conduction following treatment with heptanol: a multi-electrode array study in Langendorff-perfused mouse hearts

Running title: Conduction heterogeneities in heptanol-treated mouse hearts

Xiuming Dong MS [1], Gary Tse MD PhD FRCP [2, 3, 4], Guoliang Hao PhD [1,5], Yimei Du PhD [6]

[1] Henan SCOPE Research Institute of Electrophysiology Co. Ltd., Kaifeng 475000, China

[2] Cardiac Electrophysiology Unit, Cardiovascular Analytics Group, Hong Kong, China-UK Collaboration

[3] Tianjin Key Laboratory of Ionic-Molecular Function of Cardiovascular Disease, Department of Cardiology, Tianjin Institute of Cardiology, Second Hospital of Tianjin Medical University, Tianjin 300211, China

[4] Kent and Medway Medical School, Canterbury, UK

[5] Burdon Sanderson Cardiac Science Centre and BHF Centre of Research Excellence, Department of Physiology, Anatomy and Genetics, University of Oxford, Oxford OX1 3PT, UK

[6] Department of Cardiology, Union Hospital, Tongji Medical College, Huazhong University of Science and Technology, Wuhan, Hubei 430022, China

Keywords: action potential duration; variability; entropy; detrended fluctuation analysis; hypokalaemia

Correspondence to

Prof. Yimei Du, PhD
Research Center of Ion Channelopathy, Institute of Cardiology, Union Hospital, Tongji Medical College, Huazhong University of Science and Technology, Wuhan, China
Email: yimeidu@mail.hust.edu.cn

 doi:10.20944/preprints202205.0153.v1

Abstract

Background: Previous studies have associated slowed ventricular conduction in the arrhythmogenesis mediated by the gap junction and sodium channel inhibitor heptanol in mouse hearts but did not study the propagation patterns that might contribute to the arrhythmic substrate. This study used a multi-electrode array mapping technique, to further investigate different conduction abnormalities in Langendorff-perfused mouse hearts exposed to 0.1 or 2 mM heptanol.

Methods: Multi-electrode array recordings were made from the left ventricular epicardium in spontaneously beating hearts, during right ventricular regular 8 Hz pacing or S1S2 pacing.

Results: In spontaneously beating hearts, heptanol at 0.1 and 2 mM significantly reduced the heart rate from 314±25 to 189±24 and 157±7 bpm, respectively (ANOVA, $P<0.05$ and $P<0.001$). During regular 8 Hz pacing, Mean LATs were increased by 0.1 and 2 mM heptanol from 7.1±2.2 ms to 19.9±5.0 ms ($P<0.05$) and 18.4±5.7 ms ($P<0.05$). The standard deviation of mean LATs was increased from 2.5±0.8 ms to 10.3±4.0 ms and 8.0±2.5 ms ($P< 0.05$), and the median of phase differences was significantly increased from 1.7±1.1 ms to 13.9±7.8 ms and 12.1±5.0 ms by 0.1 and 2 mM heptanol ($P<0.05$). P_5 took a value of 0.2±0.1 ms and was not significantly altered by heptanol at 0.1 or 2 mM (1.1±0.9 ms and 0.9±0.5 ms, $P>0.05$). P_{50} was increased from 7.3±2.7 ms to 24.0±12.0 ms by 0.1 mM heptanol and then to 22.5±7.5 ms by 2 mM heptanol ($P< 0.05$). P_{95} was increased from 1.7±1.1 ms to 13.9±7.8 ms by 0.1 mM heptanol and to 12.1±5.0 ms by 2 mM heptanol ($P<0.05$). These changes led to increases in the absolute inhomogeneity in conduction (P_{5-95}) from 7.1±2.6 ms to 31.4±11.3 ms, 2 mM: 21.6±7.2 ms, respectively ($P<0.05$). The inhomogeneity index (P_{5-95}/P_{50}) was significantly reduced from 3.7±1.2 to 3.1±0.8 by 0.1 mM and then to 3.3±0.9 by 2 mM heptanol ($P<0.05$).

Conclusion: Increased activation latencies, reduced CVs and increased dispersion index of conduction were associated with both spontaneous and induced ventricular arrhythmias.

Keywords: conduction; heterogeneity; inhomogeneity; dispersion; mouse; heptanol

 doi:10.20944/preprints202205.0153.v1

Introduction

Gap junctions and sodium channels are the main factors governing the conduction velocity (CV) of cardiac action potentials (APs) travelling through heart [1-4]. Heptanol is a drug that uncouples gap junctions at concentrations < 2 mM and additionally inhibits sodium channels > 2 mM [5]. It has previously been used to explore the contributions of conduction abnormalities to ventricular arrhythmogenesis in different animal models [6, 7]. In our previous work, we associated the arrhythmogenic effects of heptanol to reduced conduction velocities (CVs) [8], abnormalities in action potential duration (APD) and CV restitution [9], as well as alterations in beat-to-beat repolarization variability in repolarization using monophasic action potential (MAP) recordings [10, 11]. However, CV was reduced by similar extents in arrhythmic and non-arrhythmic hearts, which would suggest other factors were predisposing to arrhythmogenesis. We hypothesized that increased conduction heterogeneities may be a factor, but the use of MAP recordings does not allow visualization or the measurement of local activation and propagation through the myocardium or recording from multiple sites simultaneously [12]. By contrast, the multielectrode array allows simultaneous recording of electrical activity from multiple sites at the same time, and reconstruction of activation maps from the recorded signals [13]. Therefore, this study used a multi-electrode array mapping technique, to further investigate the different conduction abnormalities in Langendorff-perfused mouse hearts exposed to 0.1 or 2 mM heptanol.

Materials and Methods

Solutions

Krebs-Henseleit solution (composition in mM: NaCl 119, $NaHCO_3$ 25, KCl 4, KH_2PO_4 1.2, $MgCl_2$ 1, $CaCl_2$ 1.8, glucose 10 and sodium pyruvate 2, pH 7.4), which has been bicarbonate-buffered and bubbled with 95% O_2–5% CO_2, was used in the experiments described in this study. Heptanol

 doi:10.20944/preprints202205.0153.v1

(Sigma, Dorset, UK; density: 0.82 g ml^{-1}) is an agent that remains soluble in aqueous solutions up to 9 mM (The Merck Index, New Jersey, USA). Krebs-Henseleit solution was used to dilute the heptanol solution to produce a final concentration of 0.1 mM.

Preparation of Langendorff-perfused mouse hearts

All experiments involving animals were approved by the Animal Research Ethics Committee of Tongji Medical College, Huazhong University of Science and Technology (IACUC Number: 2307) and were carried out in accordance with the National Institutes of Health Guide for the Care and Use of Laboratory Animals (NIH Publication, revised 2011). Male C57BL/6 mice were purchased from Vital River Laboratories, Beijing, China. Mice between 5 and 7 months of age were used. They were maintained at room temperature (21 ± 1°C) and were subjected to a 12:12 h light / dark cycle with free access to sterile rodent chow and water in an animal facility. Mice were anesthetized with isoflurane. The hearts were removed from their chest cavities and then submerged in ice-cold Krebs-Henseleit solution. The aortas were cannulated using a custom-made 21-gauge cannula prefilled with ice-cold buffer. A micro-aneurysm clip was used to secure the hearts onto the Langendorff perfusion system. Retrograde perfusion was carried out at a flow rate of 2 to 2.5 ml min^{-1} by use of a peristaltic pump. The perfusate passed through successively 200 and 5 μm filters and warmed to 37°C using a water jacket and circulator before arriving at the aorta. Approximately 90% of the hearts regained their pink colour and spontaneous rhythmic activity. These were therefore studied further. The remaining 10% did not and were discarded. The hearts were perfused for a further 20 minutes to minimise residual effects of endogenous catecholamine release, before their electrophysiology properties were characterized.

Stimulating and recording procedures

 doi:10.20944/preprints202205.0153.v1

Paired platinum electrodes (1 mm interpole distance) were used to stimulate the right ventricular epicardium electrically. This took place at 8 Hz, using square wave pulses of 2 ms in duration, with a stimulation voltage set to three times the diastolic threshold immediately after the start of perfusion. The multielectrode array, which consisted of 64 electrodes (Teflon-coated silver wires; 0.125-mm diameter; Science Products), was arranged in an 8 x 8 configuration (grid dimensions: 1.5 mm x 1.5 mm; electrode diameter: 0.1 mm; inter-electrode distance: 0.21 mm). Signals were acquired at 1.5 kHz, amplified (100 times), and digitized with 4 PXI-6031E cards (National Instrument Inc). The array was placed against either the LV surface with channel 1 near the base of the heart and channel 57 near the apex. The position of the array was determined in a consistent manner using the anatomical landmarks of the left anterior descending artery, the aorta, and the atria. Unipolar electrogram recordings were made from hearts during spontaneous activity, 8 Hz pacing and S1S2 stimulation. A reference electrode was placed on the opposite ventricle distant from the recording sites. The electrical signals were stored offline and subsequently analyzed using MappingLab EMapScope (Version 4.0). Isochrones were drawn using the built-in function of the programme. From these recordings, the following parameters were obtained: (1) local activation times (LATs), defined as the point of maximal negative slope and displayed in a grid representing the layout of the original recording array [14]. Mean values were taken from five cardiac cycles for each channel, and an overall mean value were taken from all 64 channels. Mean values from all hearts were then averaged; (2) standard deviation of the mean LATs averaged over five cardiac cycles, across 64 channels was calculated; (3) median values of histogram of the local maximum phase differences (P_{50}). (4) absolute inhomogeneity in conduction ($P_{5\text{-}95}$); (5) inhomogeneity index given by $P_{5\text{-}95}/P_{50}$ [15] and (6) P_{50}, $P_{5\text{-}95}$ and $P_{5\text{-}95}/P_{50}$ normalized to 1 mm.

Statistical analysis

 doi:10.20944/preprints202205.0153.v1

All values were expressed as mean ± standard error of the mean (SEM). Numerical data were compared by one-way analysis of variance (ANOVA). $P < 0.05$ was considered statistically significant and was denoted by * in the figures.

Results

A multi-electrode array was used to investigate the activation patterns of the LV epicardium under different pharmacological conditions. A diagram of the 64-channel multi-electrode array organized in an 8 x 8 configuration is shown in **Figure 1**. From each channel, a unipolar electrogram is recorded from spontaneously beating hearts, or during 8 Hz or S1S2 stimulation applied to the RV epicardium.

Representative traces of the electrograms recorded from spontaneously beating hearts under control conditions showed regular activity (**Figure 2**, *top panel*). In the presence of 0.1 mM heptanol, ventricular arrhythmias can be detected (**Figure 2**, *middle panel*). At 2 mM heptanol, regular activity was seen (**Figure 2**, *bottom panel*). Enlarged traces from a single channel are shown in **Figure 3A**, whereas the activation maps are shown in **Figure 3B** for 0.1 mM heptanol. For 2 mM heptanol, the traces are shown in **Figure 3C** and **Figure 3D**, respectively. Heptanol at 0.1 and 2 mM significantly reduced the spontaneous heart rate from 314 ± 25 to 189 ± 24 and 157 ± 7 bpm, respectively (ANOVA, $P < 0.05$ and $P < 0.001$; **Figure 3E**).

Subsequent experiments used 8 Hz pacing to further investigate the electrophysiological properties. The representative traces of the electrograms obtained under control conditions and in the presence of 0.1 mM or 2 mM heptanol are shown in **Figure 4**. Enlarged traces from a single channel are shown in **Figure 5A**, whereas the activation maps are shown in **Figure 5B** for 0.1 mM heptanol. For 2 mM heptanol, the traces are shown in **Figure 5C** and **Figure 5D**, respectively.

Preprints (www.preprints.org) | NOT PEER-REVIEWED | Posted: 11 May 2022 doi:10.20944/preprints202205.0153.v1

Mean LATs were increased by 0.1 and 2 mM heptanol from 7.1 ± 2.2 ms to 19.9 ± 5.0 ms (ANOVA, $P < 0.05$) and 18.4 ± 5.7 ms (ANOVA, $P < 0.05$), respectively (**Figure 6A**). The standard deviation of mean LATs was increased from 2.5 ± 0.8 ms to 10.3 ± 4.0 ms and 8.0 ± 2.5 ms, respectively (ANOVA, $P < 0.05$; **Figure 6B**), and the median of phase differences was significantly increased from 1.7 ± 1.1 ms to 13.9 ± 7.8 ms and 12.1 ± 5.0 ms by 0.1 and 2 mM heptanol (ANOVA, $P < 0.05$; **Figure 6C**). P_5 took a value of 0.2 ± 0.1 ms and was not significantly altered by heptanol at 0.1 or 2 mM (1.1 ± 0.9 ms and 0.9 ± 0.5 ms, respectively, $P > 0.05$; **Figure 6D**). By contrast, P_{50} was increased from 7.3 ± 2.7 ms to 24.0 ± 12.0 ms by 0.1 mM heptanol and then to 22.5 ± 7.5 ms by 2 mM heptanol (**Figure 6E**). P_{95} was increased from 1.7 ± 1.1 ms to 13.9 ± 7.8 ms by 0.1 mM heptanol and then to 12.1 ± 5.0 ms by 2 mM heptanol (**Figure 6F**) (ANOVA, $P < 0.05$ for all). These changes led to increases in the absolute inhomogeneity in conduction (P_{5-95}) from 7.1 ± 2.6 ms to 31.4 ± 11.3 ms, 2 mM: 21.6 ± 7.2 ms, respectively (ANOVA, $P < 0.05$; **Figure 6G**). The absolute inhomogeneity was then divided by the median to determine inhomogeneity independent of conduction velocity, yielding the inhomogeneity index (P_{5-95}/P_{50}). This index was significantly reduced from 3.7 ± 1.2 to 3.1 ± 0.8 by 0.1 mM and then to 3.3 ± 0.9 by 2 mM heptanol (ANOVA, $P < 0.05$) (**Figure 6H**).

The different measures of inhomogeneity are also normalized per unit of distance in milimetres. Thus, the normalized median of phase differences under control conditions was 4.0 ± 2.6 ms/mm and was increased to 32.5 ± 18.1 ms/mm and 28.2 ± 11.7 ms/mm by 0.1 mM and 2 mM heptanol (ANOVA, $P < 0.05$ for both cases; **Figure 7A**). Normalized values of P_5 were not significantly altered by 0.1 mM heptanol (0.4 ± 0.2 ms/mm vs. 2.6 ± 2.0 ms/mm; ANOVA, $P > 0.05$) but were increased by 2 mM heptanol to 2.1 ± 1.1 ms/mm (ANOVA, $P < 0.05$; **Figure 7B**). By contrast, normalized P_{50} (**Figure 7C**) and P_{95} (**Figure 7D**) were both increased by 0.1 and 2 mM heptanol from 4.0 ± 2.6 ms/mm to 32.5 ± 18.1 ms/mm and 28.2 ± 11.7 ms, and from 17.1 ± 6.2 ms/mm to 75.9 ± 28.1 ms/mm and 52.5 ± 17.4 ms/mm, respectively (ANOVA, $P < 0.05$ for all). These changes led to increases in the normalized absolute inhomogeneity in conduction (P_{5-95}) from 16.7 ± 6.0 ms to 73.4 ± 26.4 ms/mm and 50.4 ±

 doi:10.20944/preprints202205.0153.v1

16.8 ms/mm, respectively (ANOVA, $P < 0.05$; **Figure 7E**). The absolute inhomogeneity was then divided by the median to determine inhomogeneity independent of conduction velocity, yielding the inhomogeneity index (P_{5-95}/P_{50}). This index was significantly reduced by 0.1 and 2 mM from 7.8 1.2 mm^{-1} to 3.1 ± 0.8 mm^{-1} and 3.3 ± 0.9 mm^{-1} (ANOVA, $P < 0.05$), respectively (**Figure 7F**).

Discussion

In this study, we investigated the contributions of gap junction and/or sodium channel blockade using the pharmacological agent heptanol. A multi-electrode array was used to determine the activation latencies of 64 myocardial regions simultaneously, which permitted the construction of activation maps and quantification of both spatial and temporal dispersion of conduction. The main findings are that heptanol at both 0.1 mM and 2 mM concentrations significantly increased local activation latencies (LATs) across myocardial regions, standard deviations of LATs and absolute inhomogeneity, and decreased the inhomogeneity index.

Multi-electrode arrays can simultaneously record extracellular electrograms from multiple sites. The resulting electrogram data can be used to assess spatial heterogeneities in conduction. The standard deviation of LATs of the different recording channels can be calculated to provide a crude measure of the spread in activation times [16]. To further quantify the degree of inhomogeneity, Lammers and colleagues evaluated phase differences in LATs in the rabbit atria [15]. This enabled the building of histograms of percentile scores of the total population. Theoretically, absolute inhomogeneity in conduction, reflected by P_{5-95}, can be a primary abnormality or a secondary one resulting from reduced CVs. To distinguish between these, the absolute inhomogeneity (P_{5-95}) can be divided by the median score, P_{50}, to calculate the inhomogeneity index (P_{5-95}/P_{50}). If the inhomogeneity index were unchanged, then the inhomogeneity would be due to lower conduction velocities. If it were increased, then the increased inhomogeneity would be a primary abnormality.

 doi:10.20944/preprints202205.0153.v1

Heptanol is a long-chain alcohol that decreased fluidity of cholesterol-rich membrane domains, resulting in a reduced open probability of the gap junction channels [17, 18] without influencing its unitary conductance [19]. Heptanol inhibited gap junctions reversibly with a K_D value of 0.16 mM and a Hill coefficient of 2.3 in guinea pig ventricular cell pairs [20]. In rabbit hearts, K_D value of 0.20 mM and Hill coefficient of 2.1 were determined [21]. In another study, K_D values of 0.54 mM and 1.20 mM were found using the whole cell and perforated patch recording techniques, respectively, with a Hill coefficient of 3.45 in neonatal rat cardiomyocytes. The IC_{50} value of heptanol for gap junctions is 2.21 mM in HeLa cells expressing the gap junction protein connexin 43 [22]. However, it should be recognized that heptanol at higher concentrations affects the activity of other ion channels located at the plasma membrane. In canine cardiac Purkinje cells, heptanol blocks sodium channels with an IC_{50} of 1.3 mM, with 70% and 100% inhibition at 3 mM and 10 mM, respectively [23]. Heptanol at 0.7 mM was found to reduce the amplitude and dV/dt but not the APD of monophasic action potentials in Langendorff-perfused guinea pig hearts [24]. In the squid axon, heptanol inhibited sodium channels with a K_D of 0.93 [25]. Heptanol also inhibited calcium channels at concentrations between 0.5 mM and 6 mM with an IC_{50} value of 0.75 mM, and inward rectifier potassium channels at 3 mM although IC_{50} was not provided [26].

Together, the inhibitory effects on gap junctions and sodium channels explain the conduction slowing and increased dispersion of conduction produced by heptanol [27, 28]. In the canine ventricular myocardium, heptanol at 0.5 mM and 1 mM reduced conduction velocity both in the transverse and longitudinal directions, with greater effects in the transverse direction. The authors found that 1.5 mM heptanol produced only a 7% decrease in action potential upstroke velocity (V_{max}), suggesting that its effect on the sodium current was negligible in these experimental conditions [29]. In sheep epicardial muscle, heptanol between 1.5 mM and 3 mM produced variable effects on V_{max} but consistently reduced the overall conduction velocity, suggesting an interacting effects between alterations in intercellular coupling and the direction of action potential propagation [30]. The same group found that

 doi:10.20944/preprints202205.0153.v1

heptanol applied at concentrations between 1.5 mM 3 mM reversibly produced a major decrease in conduction velocity and eventually led to conduction block when V_{max} was only reduced by 38% in isolated sheep Purkinje fibres [31]. They further reported that V_{max} at the proximal site was unaltered whilst V_{max} at the distal site was reduced by 27% following perfusion with 2 mM heptanol. However, conduction block was observed even when V_{max} was relatively normal, suggesting that the effects were mediated through alterations in intercellular resistance. These experimental findings were supported by their computer simulations which confirmed that increases in intercellular resistance led to reductions in conduction velocity even when V_{max} was not significantly altered.

Heptanol can exert varying effects on cardiac arrhythmogenicity, depending on the concentrations applied, but also on the cardiac chamber and experimental model used. Thus, heptanol at 0.5 and 1 mM exerted pro- and anti-arrhythmic effects in the infarcted canine ventricular myocardium, respectively [6]. In isolated rabbit hearts, heptanol produced arrhythmogenic effects at concentrations between 0.1 mM and 0.3 mM [21]. By contrast, in a model of reentrant ventricular tachycardia around a ring of anisotropic myocardium from Langendorff-perfused rabbit hearts, heptanol perfusion at concentrations between 1 mM and 3 mM terminated VT [32]. Interestingly, perfusion with 1 mM heptanol reduced defibrillation threshold without affecting repolarization or refractoriness properties [33]. Regional perfusion of 0.5 mM heptanol to swine induced spontaneous ventricular fibrillation and also increased the defibrillation thresholds [34]. These effects associated with impaired gap junctional conductance and increased spatial dispersion of conduction. Furthermore, pre-treatment with 1 mM heptanol protects rabbit hearts against ischaemia by reducing the infarct size [35]. Heptanol at 0.05 mM, 0.1 mM, 0.5 mM and 1 mM conferred cardioprotective effects by reducing infarct size following ischaemia and prevented the hearts from developing ventricular arrhythmias during reperfusion [36]. However, atrial fibrillation could be induced in the presence of heptanol at low concentrations of 2 μM in isolated perfused canine atria. This effect was attributed to intercellular uncoupling as V_{max} and APD restitution were unaltered [37].

 doi:10.20944/preprints202205.0153.v1

Our previous work found that 2 mM heptanol exerted anti-arrhythmic effects on the atria [38], but pro-arrhythmic effects in the ventricles [7], of isolated mouse hearts. These were attributable to relative changes between conduction and tissue refractoriness, represented by the excitation wavelength. In this study, we found higher values of absolute inhomogeneity given by P_{5-95} induced by heptanol. Moreover, the inhomogeneity index was reduced, suggesting that the inhomogeneity was lower than that expected as a result of conduction slowing. Together, our findings implicate reduced conduction velocities and increased spatial dispersion of conduction as the substrate for reentrant arrhythmias. Our findings complement previous work in a genetic mouse model of BrS, in which temporal and spatial heterogeneities could be assessed by similar multi-electrode array setups [39]. Several factors have been identified as important contributors to spatial heterogeneity in conduction, including the direction of action potential propagation, pacing rate and premature activation [15].

There are several limitations from the use of extracellular recordings from a multi-electrode array. It cannot distinguish between various mechanisms of conduction block. Nevertheless, some inferences can be made by comparing the phase maps obtained under different conditions. For example, if the inhomogeneities are observed only during premature pacing, then a possible cause is the spatial dispersion of refractoriness [40, 41]. Moreover, if the inhomogeneities are present in a single direction only, then they are likely related to tissue anisotropy in axial resistance. By contrast, if they are present in all directions, structural abnormalities may be present. Mechanical movement of the heartbeat can cause distortion on the electrical waveforms, especially for optical mapping technique [42]. By contrast, the motion artefact represents less of a problem for the multi-electrode array technique, because the electrode can move with the heart if the electrode is closely apposed to the heart surface. In our experiments, the electrode pins are made of silver and the outer casing material is made of aluminium. The recordings showed reproducible waveforms over a long period of time. Whilst motion artefact was not a significant problem, the use of flexible electrodes can reduce this problem further. For

 doi:10.20944/preprints202205.0153.v1

example, multi-electrode arrays that are composed of flexible materials, such as thin-film polymer, can maintain better conformal contact with the heart motion [43].

Conclusions

Multi-electrode array recordings demonstrated conduction abnormalities in the form of reduced CV and increased spatial dispersion of conduction induced by heptanol in Langendorff-perfused mouse hearts.

Acknowledgements

This manuscript is based on a chapter of a doctoral thesis by G.T., which has been deposited at the University of Cambridge Repository. G.T. holds sole copyright of the contents including permission for subsequent publication. This work was supported by the National Natural Science Foundation of China (82170326 and 81770328 to Y.D.).

Conflicts of Interest

None declared.

Funding

BBSRC.

References

1. Palatinus JA and Gourdie RG. Diabetes Increases Cryoinjury Size with Associated Effects on Cx43 Gap Junction Function and Phosphorylation in the Mouse Heart. *J Diabetes Res*. 2016;2016:8789617.

2. Veeraraghavan R, Lin J, Hoeker GS, Keener JP, Gourdie RG and Poelzing S. Sodium channels in the Cx43 gap junction perinexus may constitute a cardiac ephapse: an experimental and modeling study. *Pflugers Arch*. 2015;467:2093-105.
3. Chang CJ, Cheng CC, Chen YC, Kao YH, Chen SA and Chen YJ. Gap junction modifiers regulate electrical activities of the sinoatrial node and pulmonary vein: Therapeutic implications in atrial arrhythmogenesis. *Int J Cardiol*. 2016;221:529-36.
4. Veenstra RD. Gap junction heterogeneity in reentrant ventricular tachycardia. *Cardiovasc Res*. 2006;72:196-7.
5. Nelson WL and Makielski JC. Block of sodium current by heptanol in voltage-clamped canine cardiac Purkinje cells. *Circ Res*. 1991;68:977-983.
6. Callans DJ, Moore EN and Spear JF. Effect of coronary perfusion of heptanol on conduction and ventricular arrhythmias in infarcted canine myocardium. *J Cardiovasc Electrophysiol*. 1996;7:1159-71.
7. Tse G, Hothi SS, Grace AA and Huang CL. Ventricular arrhythmogenesis following slowed conduction in heptanol-treated, Langendorff-perfused mouse hearts. *J Physiol Sci*. 2012;62:79-92.
8. Tse G, Yeo JM, Tse V, Kwan J and Sun B. Gap junction inhibition by heptanol increases ventricular arrhythmogenicity by reducing conduction velocity without affecting repolarization properties or myocardial refractoriness in Langendorff-perfused mouse hearts. *Mol Med Rep*. 2016;14:4069-4074.
9. Tse G, Liu T, Li G, Keung W, Yeo JM, Fiona Chan YW, Yan BP, Chan YS, Wong SH, Li RA, Zhao J, Wu WKK and Wong WT. Effects of pharmacological gap junction and sodium channel blockade on S1S2 restitution properties in Langendorff-perfused mouse hearts. *Oncotarget*. 2017;8:85341-85352.
10. Tse G, Hao G, Lee S, Zhou J, Zhang Q, Du Y, Liu T, Cheng SH and Wong WT. Measures of repolarization variability predict ventricular arrhythmogenesis in heptanol-treated Langendorff-perfused mouse hearts. *Curr Res Physiol*. 2021;4:125-134.
11. Tse G, Du Y, Hao G, Li KHC, Chan FYW, Liu T, Li G, Bazoukis G, Letsas KP, Wu WKK, Cheng SH and Wong WT. Quantification of Beat-To-Beat Variability of Action Potential Durations in Langendorff-Perfused Mouse Hearts. *Front Physiol*. 2018;9:1578.
12. Spira ME and Hai A. Multi-electrode array technologies for neuroscience and cardiology. *Nat Nanotechnol*. 2013;8:83-94.
13. Issa ZF, Miller JM and Zipes DP. Chapter 6 - Advanced Mapping and Navigation Modalities. In: Z. F. Issa, J. M. Miller and D. P. Zipes, eds. *Clinical Arrhythmology and Electrophysiology: A Companion to Braunwald's Heart Disease (Second Edition)* Philadelphia: W.B. Saunders; 2012: 111-143.
14. Davies L, Jin J, Shen W, Tsui H, Shi Y, Wang Y, Zhang Y, Hao G, Wu J, Chen S, Fraser JA, Dong N, Christoffels V, Ravens U, Huang CL, Zhang H, Cartwright EJ, Wang X and Lei M. Mkk4 is a negative regulator of the transforming growth factor beta 1 signaling associated with atrial remodeling and arrhythmogenesis with age. *J Am Heart Assoc*. 2014;3:e000340.
15. Lammers WJ, Schalij MJ, Kirchhof CJ and Allessie MA. Quantification of spatial inhomogeneity in conduction and initiation of reentrant atrial arrhythmias. *Am J Physiol*. 1990;259:H1254-63.
16. Zhang Y, Guzadhur L, Jeevaratnam K, Salvage SC, Matthews GDK, Lammers WJ, Lei M, Huang CLH and Fraser JA. Arrhythmic substrate, slowed propagation and increased dispersion in conduction direction in the right ventricular outflow tract of murine Scn5a+/- hearts. *Acta Physiol (Oxf)*. 2014;211:559-573.
17. Bastiaanse EM, Jongsma HJ, van der Laarse A and Takens-Kwak BR. Heptanol-induced decrease in cardiac gap junctional conductance is mediated by a decrease in the fluidity of membranous cholesterol-rich domains. *J Membr Biol*. 1993;136:135-45.

18. Takens-Kwak BR, Jongsma HJ, Rook MB and Van Ginneken AC. Mechanism of heptanol-induced uncoupling of cardiac gap junctions: a perforated patch-clamp study. *Am J Physiol*. 1992;262:C1531-8.
19. Burt JM and Spray DC. Single-channel events and gating behavior of the cardiac gap junction channel. *Proc Natl Acad Sci U S A*. 1988;85:3431-4.
20. Rudisuli A and Weingart R. Electrical properties of gap junction channels in guinea-pig ventricular cell pairs revealed by exposure to heptanol. *Pflugers Arch*. 1989;415:12-21.
21. Keevil VL, Huang CL, Chau PL, Sayeed RA and Vandenberg JI. The effect of heptanol on the electrical and contractile function of the isolated, perfused rabbit heart. *Pflugers Arch*. 2000;440:275-82.
22. Burnham MP, Sharpe PM, Garner C, Hughes R, Pollard CE and Bowes J. Investigation of connexin 43 uncoupling and prolongation of the cardiac QRS complex in preclinical and marketed drugs. *Br J Pharmacol*. 2014;171:4808-19.
23. Nelson WL and Makielski JC. Block of sodium current by heptanol in voltage-clamped canine cardiac Purkinje cells. *Circ Res*. 1991;68:977-83.
24. Caillier B, Pilote S, Castonguay A, Patoine D, Menard-Desrosiers V, Vigneault P, Hreiche R, Turgeon J, Daleau P, De Koninck Y, Simard C and Drolet B. QRS widening and QT prolongation under bupropion: a unique cardiac electrophysiological profile. *Fundam Clin Pharmacol*. 2012;26:599-608.
25. Haydon DA and Urban BW. The action of alcohols and other non-ionic surface active substances on the sodium current of the squid giant axon. *J Physiol*. 1983;341:411-27.
26. Niggli E, Rudisuli A, Maurer P and Weingart R. Effects of general anesthetics on current flow across membranes in guinea pig myocytes. *Am J Physiol*. 1989;256:C273-81.
27. Spray DC and Burt JM. Structure-activity relations of the cardiac gap junction channel. *Am J Physiol*. 1990;258:C195-205.
28. Dhein S. Pharmacology of gap junctions in the cardiovascular system. *Cardiovasc Res*. 2004;62:287-98.
29. Balke CW, Lesh MD, Spear JF, Kadish A, Levine JH and Moore EN. Effects of cellular uncoupling on conduction in anisotropic canine ventricular myocardium. *Circ Res*. 1988;63:879-92.
30. Delmar M, Michaels DC, Johnson T and Jalife J. Effects of increasing intercellular resistance on transverse and longitudinal propagation in sheep epicardial muscle. *Circ Res*. 1987;60:780-5.
31. Jalife J, Sicouri S, Delmar M and Michaels DC. Electrical uncoupling and impulse propagation in isolated sheep Purkinje fibers. *Am J Physiol*. 1989;257:H179-89.
32. Brugada J, Mont L, Boersma L, Kirchhof C and Allessie MA. Differential effects of heptanol, potassium, and tetrodotoxin on reentrant ventricular tachycardia around a fixed obstacle in anisotropic myocardium. *Circulation*. 1991;84:1307-18.
33. Qi X, Varma P, Newman D and Dorian P. Gap junction blockers decrease defibrillation thresholds without changes in ventricular refractoriness in isolated rabbit hearts. *Circulation*. 2001;104:1544-9.
34. Sims JJ, Schoff KL, Loeb JM and Wiegert NA. Regional gap junction inhibition increases defibrillation thresholds. *Am J Physiol Heart Circ Physiol*. 2003;285:H10-6.
35. Saltman AE, Aksehirli TO, Valiunas V, Gaudette GR, Matsuyama N, Brink P and Krukenkamp IB. Gap junction uncoupling protects the heart against ischemia. *J Thorac Cardiovasc Surg*. 2002;124:371-6.
36. Chen BP, Mao HJ, Fan FY, Bruce IC and Xia Q. Delayed uncoupling contributes to the protective effect of heptanol against ischaemia in the rat isolated heart. *Clin Exp Pharmacol Physiol*. 2005;32:655-62.
37. Ohara T, Qu Z, Lee MH, Ohara K, Omichi C, Mandel WJ, Chen PS and Karagueuzian HS. Increased vulnerability to inducible atrial fibrillation caused by partial cellular uncoupling with heptanol. *Am J Physiol Heart Circ Physiol*. 2002;283:H1116-22.

 doi:10.20944/preprints202205.0153.v1

38. Tse G, Tse V, Yeo JM and Sun B. Atrial Anti-Arrhythmic Effects of Heptanol in Langendorff-Perfused Mouse Hearts. *PLoS One*. 2016;11:e0148858.
39. Jeevaratnam K, Poh Tee S, Zhang Y, Rewbury R, Guzadhur L, Duehmke R, Grace AA, Lei M and Huang CL. Delayed conduction and its implications in murine Scn5a(+/-) hearts: independent and interacting effects of genotype, age, and sex. *Pflugers Arch*. 2011;461:29-44.
40. Boineau JP, Schuessler RB, Mooney CR, Miller CB, Wylds AC, Hudson RD, Borremans JM and Brockus CW. Natural and evoked atrial flutter due to circus movement in dogs. Role of abnormal atrial pathways, slow conduction, nonuniform refractory period distribution and premature beats. *Am J Cardiol*. 1980;45:1167-81.
41. Allessie MA, Bonke FI and Schopman FJ. Circus movement in rabbit atrial muscle as a mechanism of tachycardia. II. The role of nonuniform recovery of excitability in the occurrence of unidirectional block, as studied with multiple microelectrodes. *Circ Res*. 1976;39:168-77.
42. Brack KE, Narang R, Winter J and Ng GA. The mechanical uncoupler blebbistatin is associated with significant electrophysiological effects in the isolated rabbit heart. *Experimental Physiology*. 2013;98:1009-1027.
43. Rajendran Pradeep S, Ajijola Olujimi A, Vetter R, Snellings A, Tompkins John D, Deb A, Kipke Daryl R, Shivkumar K and Ardell Jeffrey L. Abstract 16717: Customizable High-density Microelectrode Arrays for Murine Cardiac Electrophysiology. *Circulation*. 2016;134:A16717-A16717.

Preprints (www.preprints.org) | NOT PEER-REVIEWED | Posted: 11 May 2022 doi:10.20944/preprints202205.0153.v1

Figures

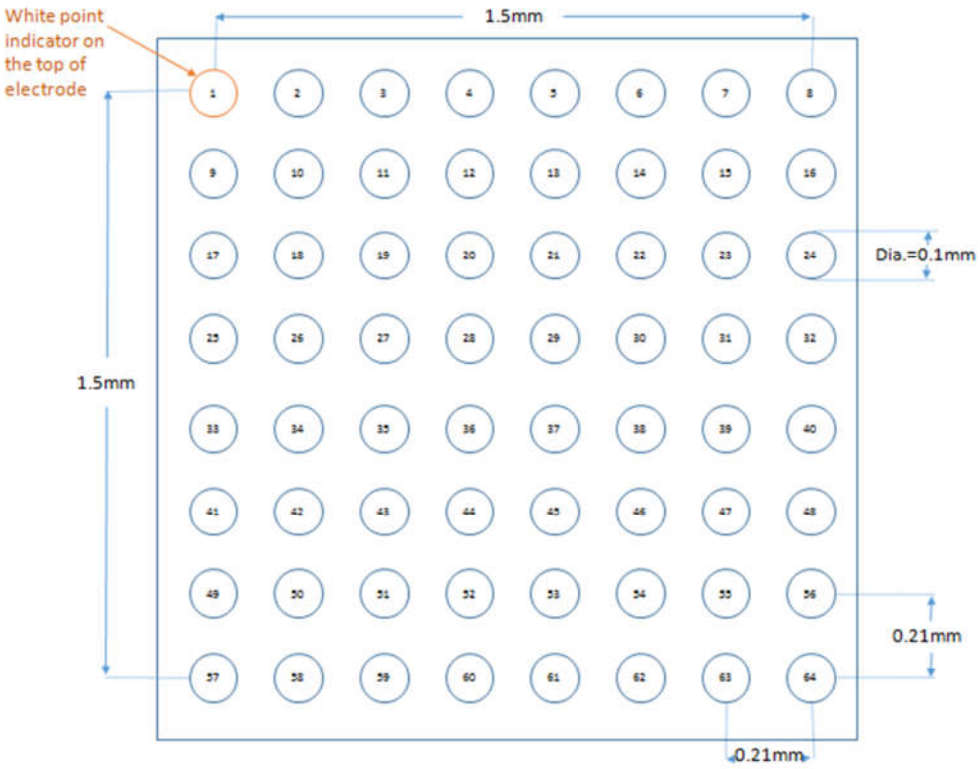

Figure 1. A cartoon of 64-channel multi-electrode array arranged in an 8 x 8 grid.

Preprints (www.preprints.org) | NOT PEER-REVIEWED | Posted: 11 May 2022 doi:10.20944/preprints202205.0153.v1

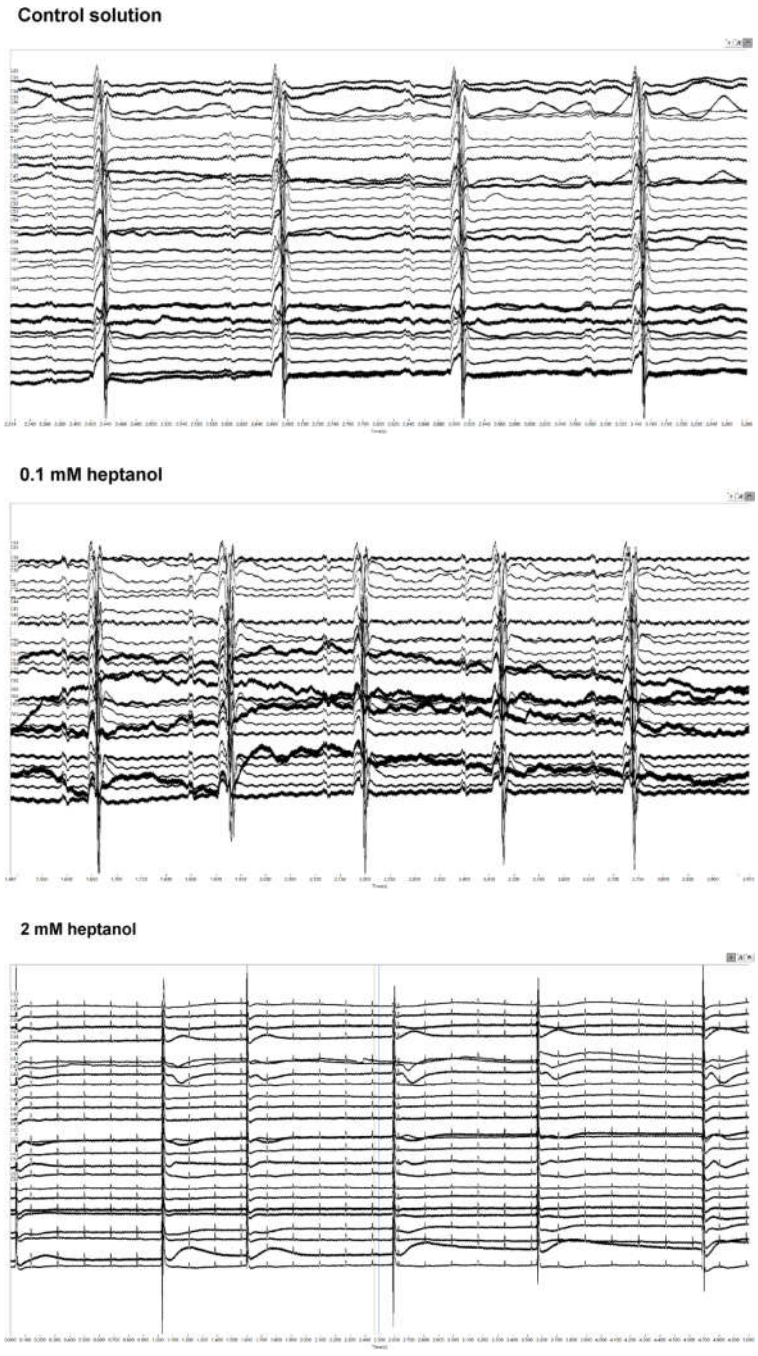

Figure 2. Representative biphasic electrograms obtained from spontaneously beating hearts under control conditions (*top*) and in the presence of 0.1 mM (*middle*) or 2 mM heptanol (*bottom*).

Preprints (www.preprints.org) | NOT PEER-REVIEWED | Posted: 11 May 2022 doi:10.20944/preprints202205.0153.v1

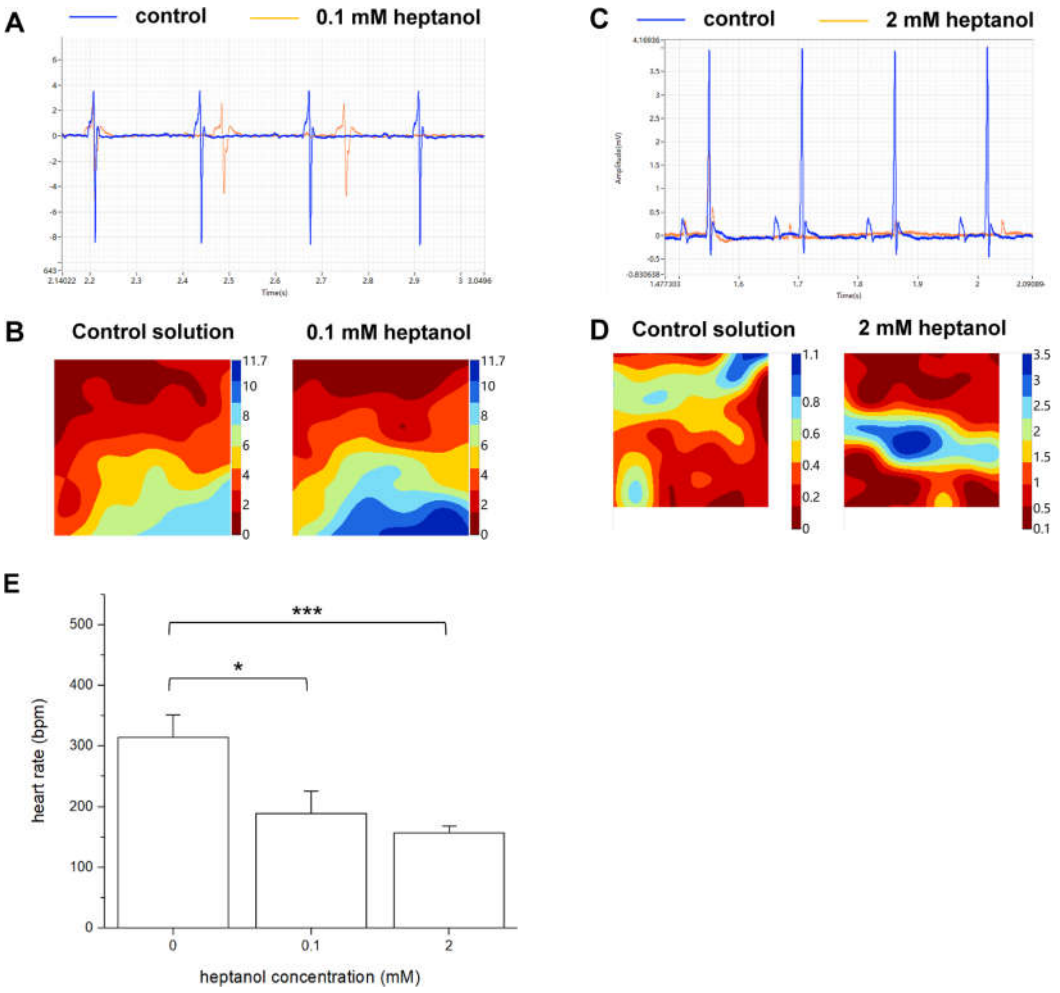

Figure 3. Representative biphasic electrograms from a single channel (A) and corresponding activation maps (B) obtained from spontaneously beating hearts under control conditions and in the presence of 0.1 mM. Representative biphasic electrograms from a single channel (C) and corresponding activation maps (D) obtained from spontaneously beating hearts under control conditions and in the presence of 2 mM. There was a dose-dependent reduction in heart rate as heptanol concentration increased (E). * $P<0.05$, *** $P<0.001$. Data from n=5 hearts. Differences between groups were tested using ANOVA followed by Tukey's honestly significant difference test.

Preprints (www.preprints.org) | NOT PEER-REVIEWED | Posted: 11 May 2022 doi:10.20944/preprints202205.0153.v1

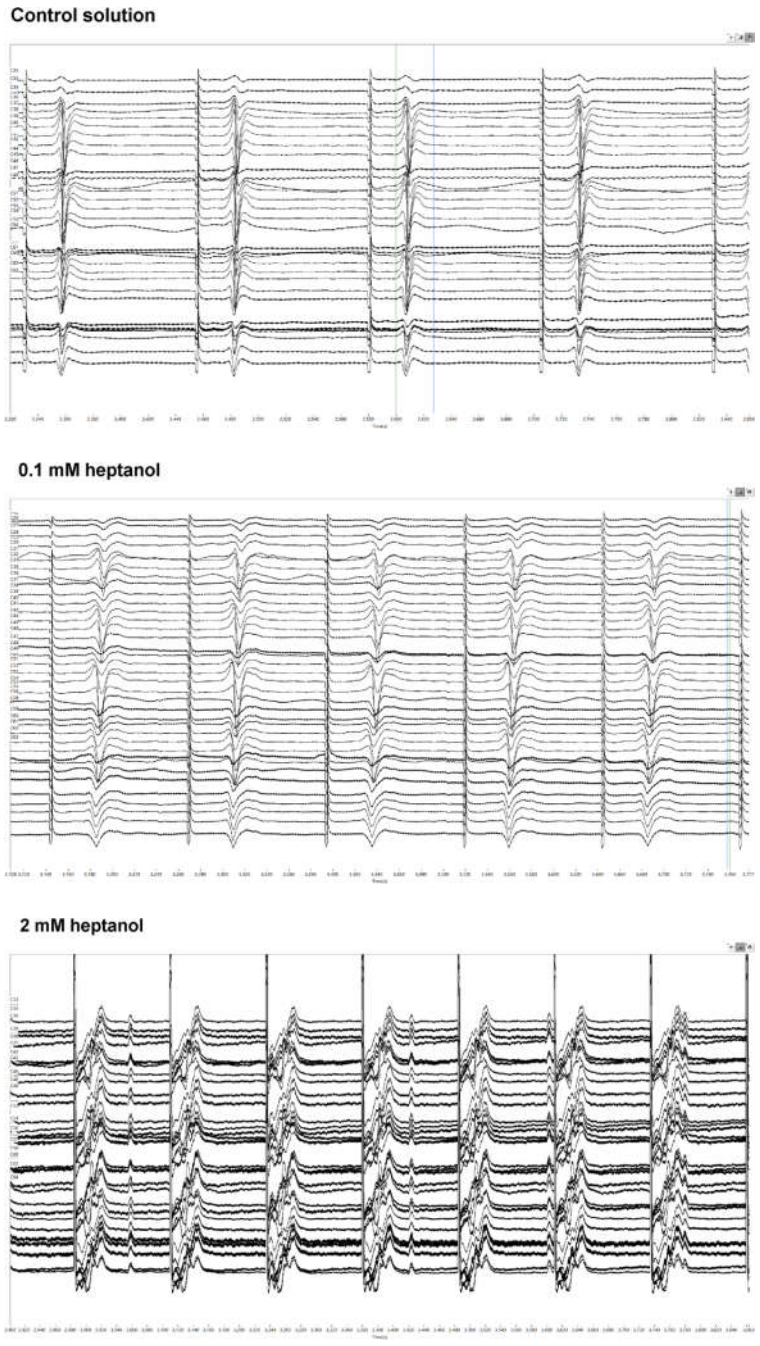

Figure 4. Representative biphasic electrograms obtained during 8 Hz pacing under control conditions (*top*) and in the presence of 0.1 mM (*middle*) or 2 mM heptanol (*bottom*).

Preprints (www.preprints.org) | NOT PEER-REVIEWED | Posted: 11 May 2022 doi:10.20944/preprints202205.0153.v1

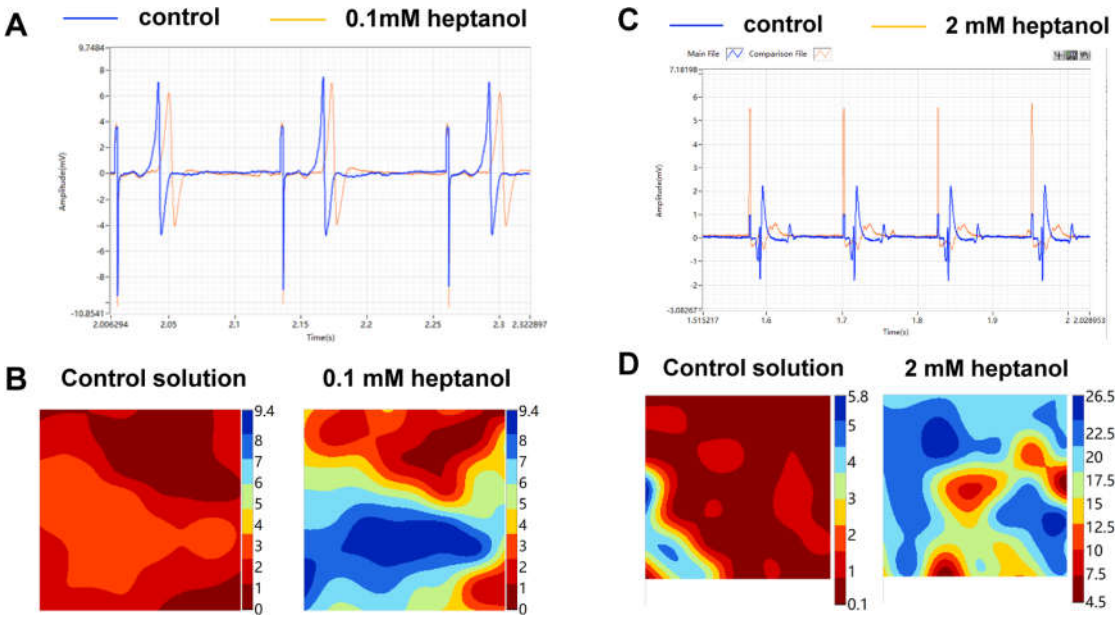

Figure 5. Representative biphasic electrograms (A) and corresponding activation maps (B) from a single channel obtained during 8 Hz pacing under control conditions and in the presence of 0.1 mM. Representative biphasic electrograms (C) and corresponding activation maps (D) from a single channel obtained during 8 Hz pacing under control conditions and in the presence of 2 mM.

Preprints (www.preprints.org) | NOT PEER-REVIEWED | Posted: 11 May 2022 doi:10.20944/preprints202205.0153.v1

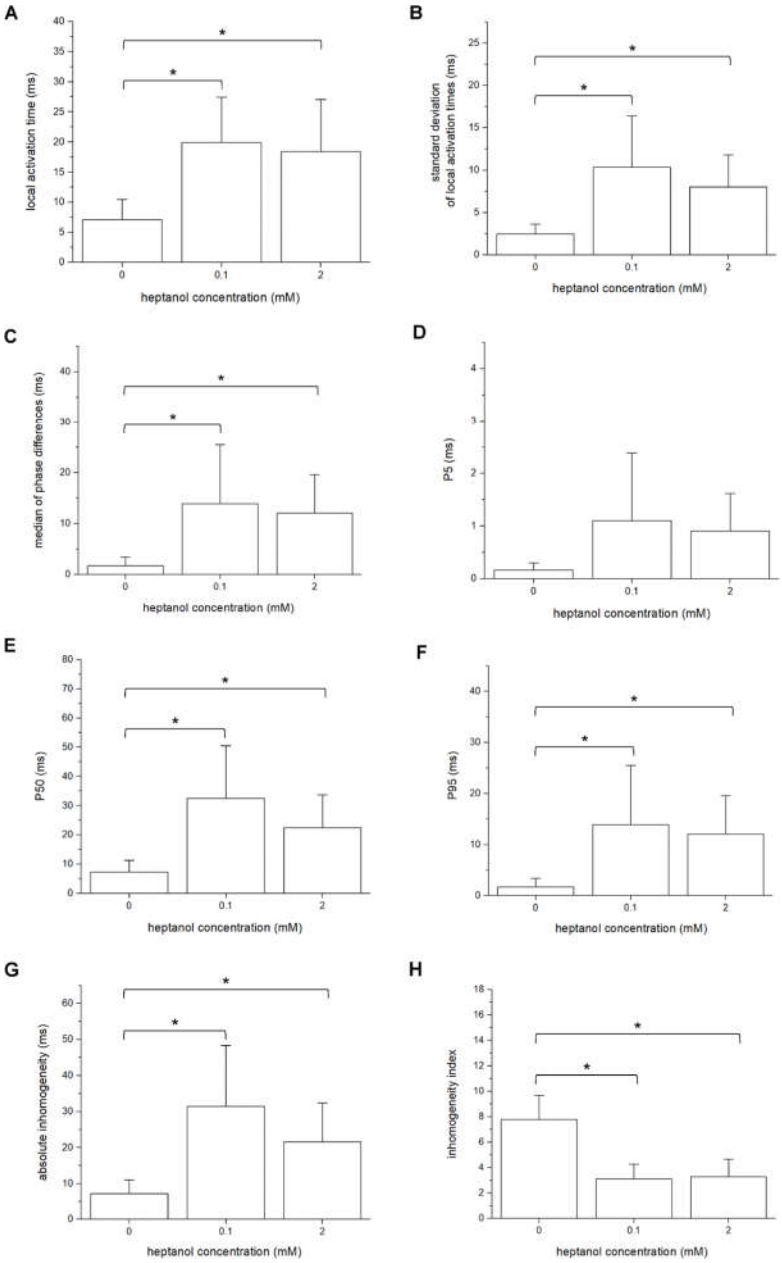

Figure 6. Mean local activation time (LAT) (A), standard deviation of mean LATs (B), median of phase differences (C), P_5 (D), P_{50} (E), P_{95} (F), absolute inhomogeneity (P_{5-95}, G) and inhomogeneity index (P_{5-95}/P_{50}, H) obtained during 8 Hz pacing before and after introduction of 0.1 mM or 2 mM heptanol. Data from n=5 hearts. Differences between groups were tested using ANOVA followed by Tukey's honestly significant difference test.

Preprints (www.preprints.org) | NOT PEER-REVIEWED | Posted: 11 May 2022 doi:10.20944/preprints202205.0153.v1

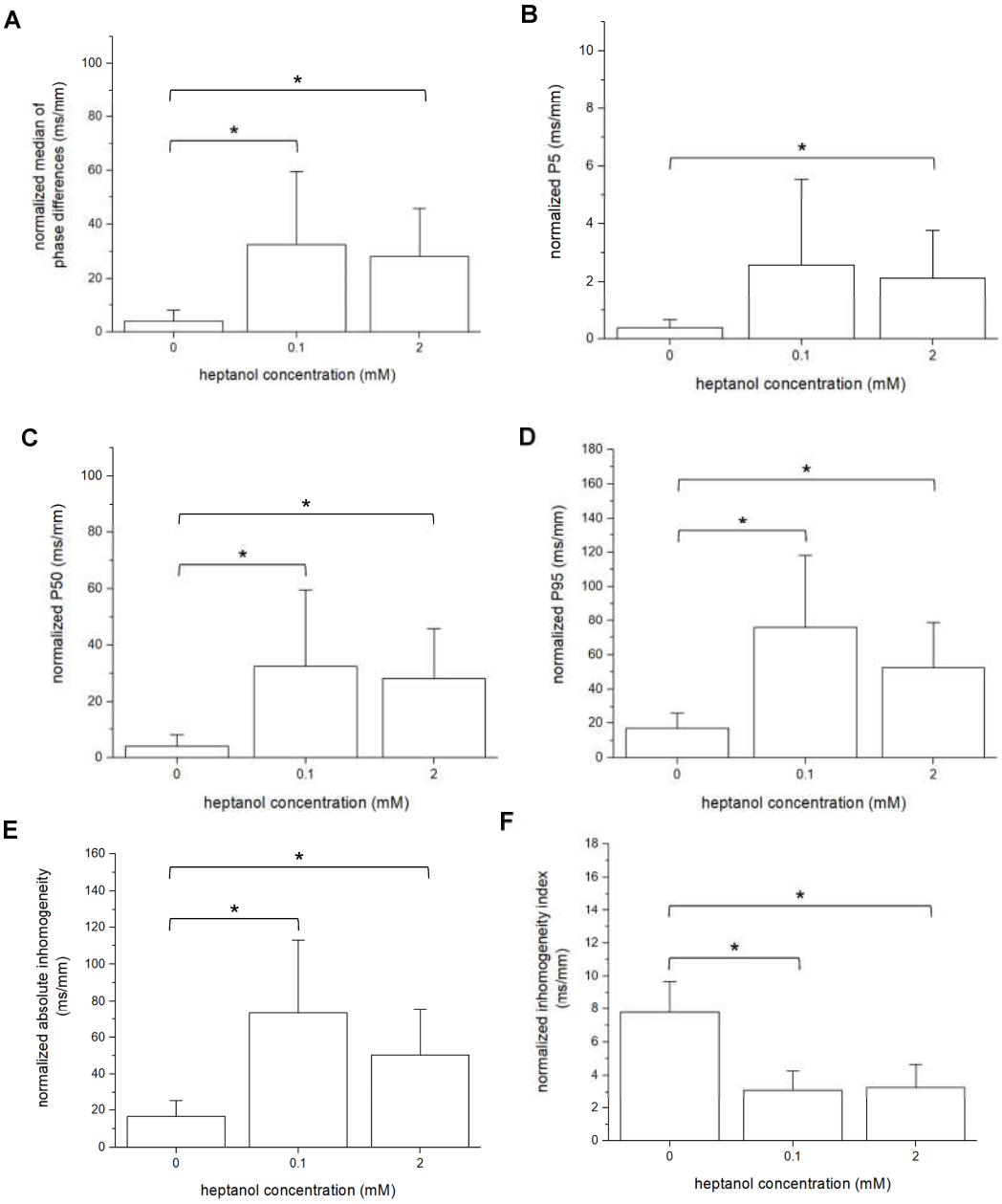

Figure 7. Normalized median of phase differences (A), P_5 (B), P_{50} (C), P_{95} (D), absolute inhomogeneity ($P_{5\text{-}95}$, E) and inhomogeneity index ($P_{5\text{-}95}/P_{50}$, F) obtained during 8 Hz pacing before and after introduction of 0.1 mM or 2 mM heptanol. Data from n=5 hearts. Differences between groups were tested using ANOVA followed by Tukey's honestly significant difference test.